Superconductivity and Electron Tunneling

Thomas McColgan and Miguel García Echevarría
Low Temperature Laboratoy, Condensed Matter Physics Department
Faculty of Science, UAM

Madrid, May 20, 2008

Abstract

We repeat the 1960 experiment by Giaver, in which the tunneling current from a superconductor through an insulating film is measured to obtain the width of its gap. Our results and the discrepancies to the BCS Theory are discussed. We measure the lead energy gap to be (1.4 ± 0.1) meV.

1 Introduction

The theory of superconductivity presented by Bardeen, Cooper and Schrieffer in 1957 predicts a gap in the allowed energies for electrons. Even though this gap had been measured indirectly by several methods, it had not been measured directly until 1960, when Giaver conducted his electron tunneling experiment. Here we report our attempt to reproduce this seminal work.
In 1973 Giaver was awarded the Nobel Prize for his achievement. This is a feat we are not attempting to reproduce here; a 10 will be sufficient...

2 Theoretical Approach

The transition rate W for an electron from an occupied state in the layer 1 with momentum $\mathbf{p_1}$ to a free state in the layer 2 with momentum $\mathbf{p_2}$ can be calculated by means of the Fermi Golden Rule like follows:

$$W^{1e}_{1\to 2} = \frac{2\pi}{\hbar}|T_{21}|^2 f(\epsilon_{\mathbf{p_1}})[1-f(\epsilon_{\mathbf{p_2}})]\delta(\epsilon_{\mathbf{p_1}}-\epsilon_{\mathbf{p_2}})\delta_{s_1 s_2}, \tag{1}$$

where T_{21} is the transition amplitud, $f(\epsilon_{\mathbf{p_1}})$ the probability that the state $\mathbf{p_1}$ is occupied and $[1 - f(\epsilon_{\mathbf{p_2}})]$ the probability that the state $\mathbf{p_f}$ is empty, and the conservation of the energy and spin in the transition are assumed.

The total transition rate from the electrode 1 to the electrode 2 will be

$$W_{1\to 2} = \frac{2\pi}{\hbar}\sum_{\substack{s_1,s_2\\ \mathbf{p_1},\mathbf{p_2}}} |T_{21}|^2 f(\epsilon_{\mathbf{p_1}})[1-f(\epsilon_{\mathbf{p_2}})]\delta(\epsilon_{\mathbf{p_1}}-\epsilon_{\mathbf{p_2}})\delta_{s_1 s_2}. \tag{2}$$

If the transition hamiltonian does not depend on the spin and couples weakly the electrodes when the applied voltage is small (a valid approximation for the voltages used in this experiment), we can simplify the expression (2):

$$W_{1\to 2} = \frac{4\pi}{\hbar}|T|^2 \sum_{\mathbf{p_1},\mathbf{p_2}} f(\epsilon_{\mathbf{p_1}})[1-f(\epsilon_{\mathbf{p_2}})]\delta(\epsilon_{\mathbf{p_1}}-\epsilon_{\mathbf{p_2}}). \tag{3}$$

The transition rate in the opposite way is analogous.

Now we can write explicitly the expression for the current in the $1 \to 2$ direction:

$$I = e\ (W_{1\to 2} - W_{2\to 1}), \tag{4}$$

that is

$$I = \frac{4\pi e}{\hbar}|T|^2 \sum_{\mathbf{p_1},\mathbf{p_2}} [f(\epsilon_{\mathbf{p_1}}) - f(\epsilon_{\mathbf{p_2}})]\delta(\epsilon_{\mathbf{p_1}} - \epsilon_{\mathbf{p_2}}).. \tag{5}$$

If we replace the summatories by integrals, considering that the momentums configure a quasicontinuum, and assuming a voltage difference V between the electrodes that makes $\mu_2 - \mu_1 = eV$, we get

$$\begin{aligned} I &= \frac{4\pi e}{\hbar}|T|^2 \times \\ &\times \int_{-\infty}^{\infty} d\epsilon\ N_1(\epsilon - eV)\ N_2(\epsilon)[f(\epsilon - eV) - f(\epsilon)], \end{aligned} \tag{6}$$

where $N(E)$ is the density of states, needed to perform the change from summatories to the integral.

Now three cases can be distinguished, that is, when both electrodes are metals in the normal

state, when only one of them is in the superconducting state and when both are in the superconducting state. The only difference between these situations is the form of the density of states $N(E)$, so it must be replaced by the adequate expression.

2.1 Normal-Normal junction

For a sufficient small voltage V, the state densities can be considered nearly constant, and equation (6) reads

$$I^{NN} = \frac{4\pi e}{\hbar}|T|^2 N_1(\mu)N_2(\mu)eV, \tag{7}$$

where we have used the fact that

$$\int_{-\infty}^{\infty} d\epsilon[f(\epsilon - eV) - f(\epsilon)] \simeq eV.$$

From this equation can be derived easily the normal conductance of the junction

$$C^{NN} = \frac{1}{R^{NN}} = \frac{dI^{NN}}{dV} = \frac{4\pi e^2}{\hbar}|T|^2 N_1(\mu)N_2(\mu). \tag{8}$$

2.2 Normal-Superconductor junction

The state density for a superconductor can be derived from considering a continuum spectrum of energy levels, and hence

$$N_N(\epsilon)d\epsilon = N_S(E)dE. \tag{9}$$

The relation between ϵ and E in the range of the BCS Theory of Superconductivity is $E_{\mathbf{p}} = \sqrt{\epsilon_{\mathbf{p}}^2 + \Delta^2}$, with Δ the gap of the superconductor. So we can get

$$\begin{aligned} N_S(E) &= N_N(\epsilon)\left|\frac{d\epsilon}{dE}\right| = \\ &= \begin{cases} N_N(\epsilon)\frac{|E|}{\sqrt{E^2-\Delta^2}}, & |E| > \Delta \\ 0, & |E| \geq \Delta \end{cases} . \end{aligned} \tag{10}$$

If we replace this state density in (6) we get the I^{NS}, but only up to $|T|^2$ order. There are high order effects by means of Cooper pair transmission to the superconducting electrode. Neglecting these issues, the current for small voltages is

$$\begin{aligned} I^{NS} &= \frac{4\pi e}{\hbar}|T|^2 N_{1N}(\mu) \times \\ \times &\int_{-\infty}^{\infty} dE\ N_{2S}(E)[f(E-eV) - f(E)] = \\ = &\frac{4\pi e}{\hbar}|T|^2 N_{1N}(\mu)N_{2N}(\mu) \times \\ \times &\int_{-\infty}^{\infty} dE\ \frac{|E|}{\sqrt{E^2-\Delta^2}}[f(E-eV) - f(E)]. \end{aligned} \tag{11}$$

It can be expressed in terms of the C^{NN} like follows:

$$I^{NS} = \frac{C^{NN}}{e}\int_{-\infty}^{\infty} dE\ \frac{|E|}{\sqrt{E^2-\Delta^2}}[f(E-eV) - f(E)]. \tag{12}$$

Finally, introducing $x = E - \Delta$ and noting that Fermi functions are even, we get the expression that is used for numerical analysis:

$$\begin{aligned} I^{NS} &= \frac{C^{NN}}{e}\int_0^{\infty} dx\ \frac{x+\Delta}{\sqrt{x(x+2\Delta)}} \times \\ &\times\ [f(x+\Delta-eV) - f(x+\Delta+eV)]. \end{aligned} \tag{13}$$

From eqrefins, the conductance will be the following

$$\begin{aligned} C^{NS} &= \frac{1}{R^{NS}} = \frac{dI^{NS}}{dV} = \\ &= \frac{C^{NN}}{e}\int_{-\infty}^{\infty} dE\ \frac{|E|}{\sqrt{E^2-\Delta^2}}\frac{\partial f(E-eV)}{\partial V} \end{aligned} \tag{14}$$

2.3 Superconductor-Superconductor junction

By analogy with the previous section, we write directly the expression of the current for this situation:

$$I^{SS} = \frac{C^{NN}}{e}\int_{-\infty}^{\infty} dE\ \frac{E^2\ [f(E-eV) - f(E)]}{\sqrt{(E^2-\Delta_1^2)}\sqrt{(E^2-\Delta_2^2)}}. \tag{15}$$

3 Experimental Method

Our aim in this experiment was to measure superconductor to normal tunneling as described above. To achieve this we choose Aluminum as the superconductor and Lead as the normal conductor. This is convenient because Al and Pb have a transition

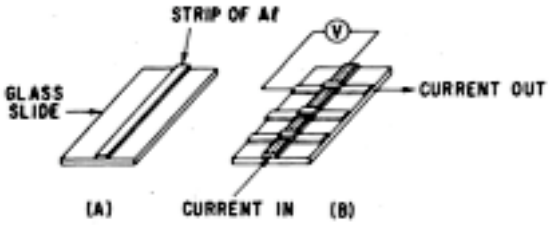

Figure 1: Hola

temperature of $1.140K$ and $7.193K$ respectively. Therefore the range in between the two allows the observation of the desired effect. Another benefit is that Aluminum readily oxidizes to Al_2O_3 at room temperature, providing an insulating layer.

3.1 Sample Preparation

Sample preparation was done in a manner similar to the one described in **??**. First a thin layer of Aluminum was vapor-deposited by means of a heated spiral filament onto a microscope slide in a vacuum chamber. Air was then let into the chamber, allowing a thin insulating film of Al_2O_3 to form. Finally the chamber was evacuated again, and the last layer, consisting of Pb, was deposited.

The layers were deposited in the shape of strips, a long strip of Al crossed by 5 shorter strips of Pb, providing up to 5 tunnel junctions per slide. The shapes of the layers were determined by placing a mask between the heated filament and the slide.

LAYER THICKNESS

There are 2 main reasons for preparing the samples in a vacuum. Firstly it is necessary to keep the layers as free from contamination as possible, because due to their thinness even small amounts of foreign substances might cause a change in behavior. Secondly the vacuum significantly reduces scattering effects, making the thickness of the deposited layers as homogenous as possible. This is necessary so that the current is distributed evenly across the junction.

We used an oil diffusion pump to attain a high vacuum of about *??* bar.

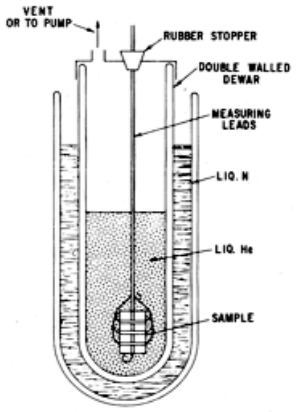

Figure 2: Hola

3.2 Measurement

The sample was immersed in a cryostat containing liquid He surrounded by a layer of liquid N. A rotary pump was connected to the cryostat to reduce pressure inside. Since the vapor pressure is linked to the Temperature of the Helium this allowed us to perform measurements at several temperatures. A mechanical manometer was also connected to the chamber.

The tunnel junction was connected in a 4 terminal configuration, i.e. the voltage and current were measured in two separate circuits, which only joined at the tunneling junction. This setup has the advantage that only the potential difference at the junction itself is measured, and factors such as the resistivity of cables leading up to the sample, and the change with temperature thereof, do not have to be taken into account.

In our setup the Ampere-meter also functioned as a current source. Both units were connected to a computer via an IEEE interface, which was used to set the current and record the readings. In each measurement run the voltage across the junction was measured for a range of equally spaced current intensities, as produced by said current source. We measured ranges from *??* to *??* using divisions between 100 and 2000 steps. A time of $1s$ was left between measurements to allow for the readings to stabilize.

The resolution of voltage measurements depended greatly on the range in which the measurement was taken. The Volt-meter automatically changes the resolution, therefor we tried to avoid such changes of resolution by setting corresponding

limits on the current. When the data contained a change of scale we omitted the data points beyond the change. The effects of this change of resolution are most severe in the numerical derivation, since this is done by dividing the differences.

CRYOSTAT GRAPHIC??

4 Results and Analysis

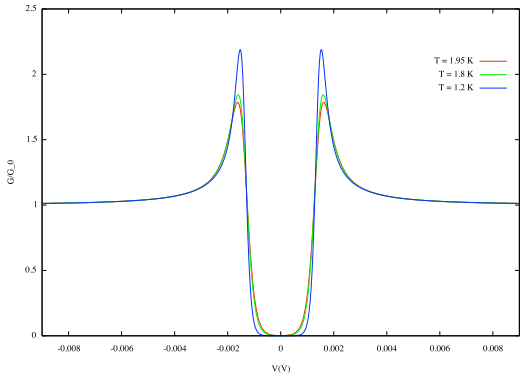

Figure 3: BCS theoretical conductance curves for different temperatures.

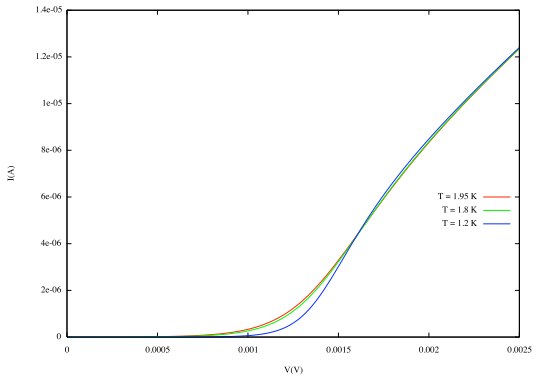

Figure 4: BCS theoretical current curves for different temperatures.

4.1 Data Analysis

Our first step in analyzing the data collected was to plot it. Since the shape of the energy spectrum is given by the derivative of the I-V curve, it was necessary to numerically calculate the derivative. The method we chose to do this was to fit a linear function to n neighboring data points using a straightforward least squares approach. The slope of the fitted function was taken as the derivative.This had the additional benefit of performing some smoothing. Of course there is some information lost in the process, but this was not deemed critical as the number of points collected was generally much larger than n.

In order to estimate the energy gap of our Pb sample it was necessary to evaluate the integral in 13, and compare the results to the experimental data. In order to do so we split the integral in 2 parts. The high energies were evaluated numerically using a Romberg-Method algorithm [1], while the lower energies were estimated analytically. It was assumed that $[f(x+\Delta-eV)-f(x+\Delta+eV)] \approx$ const. for small x, as it is finite and nonzero for $x = 0$, while the second part, $\frac{x+\Delta}{\sqrt{x(x+2\Delta)}}$ diverges for $x \to 0$. It can, however, be integrated analytically up to 0,[2]thus enabling us to efficiently integrate for all x. The resulting curve was derivated in the same manner as the experimental data, to ensure their comparability.

EdNote(1)

EdNote(2)

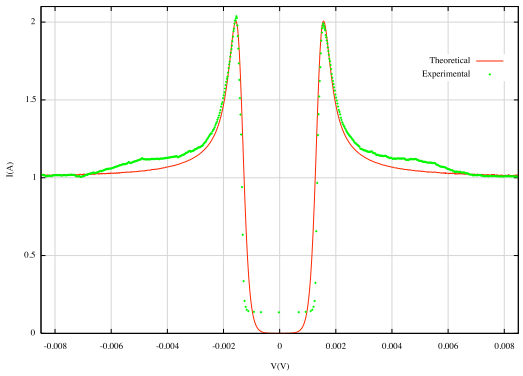

Figure 5: Experimental data and BCS theoretical prediction for $1.45K$. The different density of states of Pb with respect to BCS causes the discrepancy.

When plotting the derivatives in this way and comparing them qualitatively to each other for some arbitrary but reasonable values of T,Δ and C_{NN} it quickly becomes apparent that there are certain qualitative differences between the experimental results and the results predicted by the BCS theory. Specifically, there are some bulges in the conductance curves outside the gap in the experimental data which are not present in the theory (see fig. 5).

Our best guess as to what might be causing this effect is electron-phonon scattering. [3] It seems not

EdNote(3)

[1] EdNote: Citation for this from Num. Recipes.
[2] EdNote: perhaps the analytical integral expression here?
[3] EdNote: Add a citation for this?

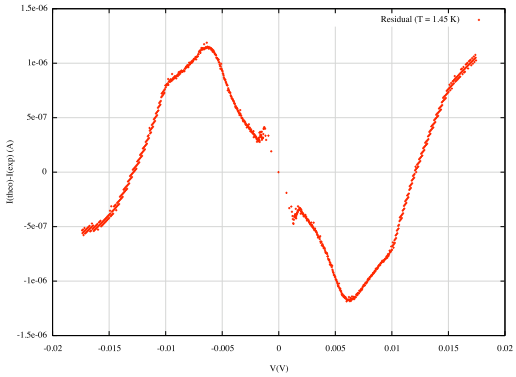

Figure 6: Residual between theoretical and experimental current curve for $1.45K$. The phonon structure arises clearly.

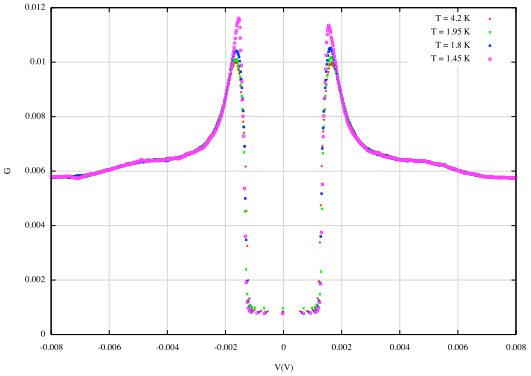

Figure 7: Measured conductance for 4 different temperatures. The peaks coincidence sustains the nearly invariance of the gap for this temperature range. The phonon structure is the same for all.

to vary significantly with Temperature(see figure 7) in the range of our observations. The shape of the deviation from the current predicted by BCS theory can be seen in figure 6.

The initial idea for estimating the energy gap and the other parameters of the model(T,C_{NN}) was to fit them using a least squares method. We tried to do so using a Levenberg-Marquard routine. This approach proved inefficient, with the results being rather dependent on the initial guess, and convergence reached at unexpected values. This is probably due to the algorithm over-fitting in the region affected by the model insufficiencies described above, as well as the high degree of nonlinearity exhibited by the function.

A more feasible method was to estimate normal-normal conductance and temperature from other measurements, and then fitting the value of the gap "by hand".

4.2 Results

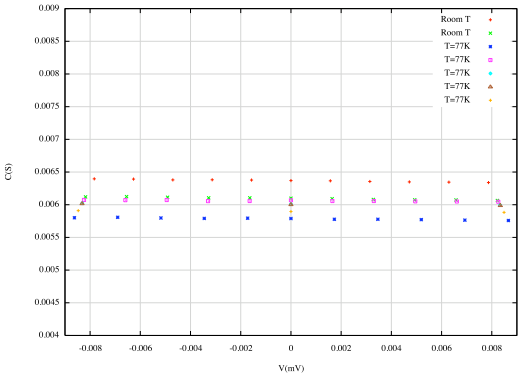

Figure 8: Conductance curves .

Prior to inserting He into the cryostat as described in[4], we measured the conductivity of the sample several times at different temperatures. From these measurements we determined $C_{NN} = 0.006 \pm 0.0005S$. The values taken in the relevant range of voltages can be seen in figure **??**. EdNote(4)

The values for the Temperature were obviously different for each measurement. We determined it by means of associating temperatures to pressures at the surface of the He^4 using the vapor pressure curve. As described earlier, there was a manometer connected to the cryostat, and readings were taken at every measurement. This assumes that the pressure is the same at the surface and at the top of the cryostat, where the measurement is taken.[5] [6] The measurements from the manometer might also have been faulty, the pressure shown at room pressure was too low. The difference caused by this miscalibration seemed to be very low at lower pressures. EdNote(5) EdNote(6)

With the other parameters now fixed, the with of the energy gap can now be fitted. Theoretically it depends on the temperature, but in the range of temperatures we measured in this change is very small, as can be seen in figure 9. The amount of change is[7], which is about the error we expected to be caused by our fitting of the value "by hand", and we consequently assumed the value to be the EdNote(7)

[4] EdNote: section reference
[5] EdNote: Why is this assumption OK
[6] EdNote: add a temperature/pressure table?
[7] EdNote: short calculation of error percentage

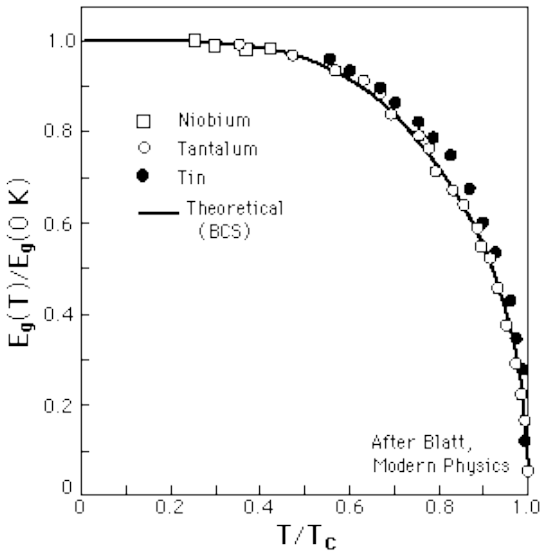

Figure 9: Reduced values of the observed energy gap as a function of the reduced temperature, after Towsend and Sutton. The solid curve is drawn for the BCS theory.

same in all the measurements. Fitting the width by this process for the different measurements gave us a value of 1.4 ± 0.1 meV. The error is a rough estimate based on the finesse with which we manually adjusted the gap. It is probably a little to large, yet we decided to give this slightly higher figure to account for the uncertainties in the temperature.

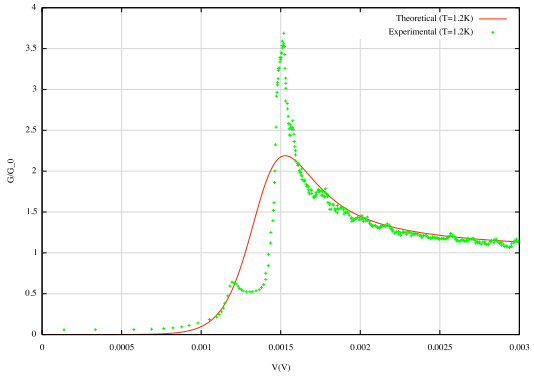

Figure 10: Experimental data and BCS theoretical prediction for $1.2K$. There is a second peak due to the superconductor transition of some parts of the Aluminum.

The measurement at the lowest temperature that we could perform gives qualitatively different results. In fig. (figure 10) can be seen the appearance of new effects. The transition temperature T_c for Aluminum is $7.193K$, and we have established experimentally the temperature for data as $1.2K$. However, due to the difference between bulk properties and those that we must consider here for films, the T_c is a little bit greater ([8]). EdNote(8)

The situation is qualitatively clear now, i.e. the temperature has fallen enough to let some portions of Aluminum change to superconducting state, creating this combined effect between normal-superconductor and superconductor-superconductor junctions. It can be explained by considering a sum of junctions of these two kinds in parallel, so as to produce an I-V curve with peaks inside the gap of the Aluminum. For a superconductor-superconductor junction appear two peaks, located at $|\Delta_1 - \Delta_2|$ and $(\Delta_1 + \Delta_2)$.

References

[1] I. Giaever and K. Megerle, *Study of Superconductors by Electron Tunneling*, Phys. Rev. vol. 122, Num. 4, p. 1101 (1961)

[2] I. Giaever, *Electron Tunneling and Superconductivity*, Rev. Mod. Phys. vol. 48, Num. 2, (1974)

[3] I. Giaever, *Energy Gap in Superconductor Measured by Electron Tunneling*, Phys. Rev. Let. vol. 5, Num. 4, p. 147 (1960)

[4] R. Frerichs and J. P. Wilson, *Tunnel-Effect Measurements on Superimposed Layers of Lead and Aluminum*, Phys. Rev. vol. 142, Num. 1, p. 264 (1966)

[5] J. Bardeen, L. N. Cooper and J. R. Schrieffer, *Theory of Superconductivity*, Phys. Rev. vol. 108, Num. 5, p. 1175 (1957)

[6] N. W. Ashcroft and N. D. Mermin, *Solid State Physics*, Harcourt College Publishers (1976)

[7] Jianping Li, *General explicit difference formulas for numerical differentiation*, Journal of Computational and Applied Mathematics vol. 183, p. 29 (2005)

[8] W. H. Press, S. A. Teukolsky, W. T. Vetterling and B. P. Flannery *Numerical Recipes*, Cambridge University Press (1997)

[8] EdNote: reference for this